Langmuir



Research Article

# Preparation of Protein–Silicate Hybrids from Polyamine Intercalation of Layered Montmorillonite

Jiang-Jen Lin, Jiun-Chiou Wei, Tzong-Yuan Juang, and Wei-Cheng Tsai

*Langmuir*, **2007**, 23 (4), 1995-1999 • DOI: 10.1021/la062013h



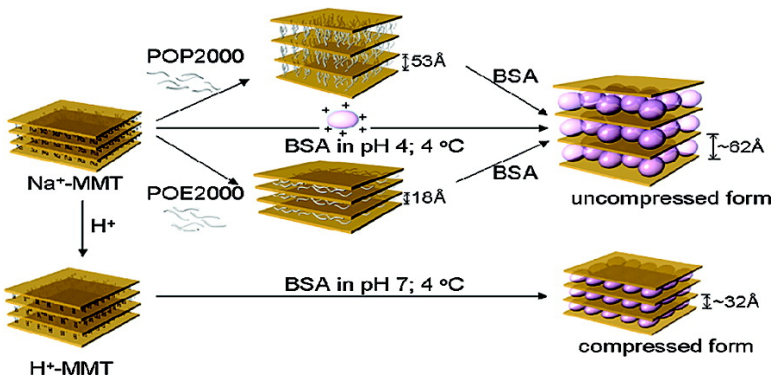


## More About This Article

Additional resources and features associated with this article are available within the HTML version:

- Supporting Information
- Links to the 4 articles that cite this article, as of the time of this article download
- Access to high resolution figures
- Links to articles and content related to this article
- Copyright permission to reproduce figures and/or text from this article

View the Full Text HTML

# Preparation of Protein−Silicate Hybrids from Polyamine Intercalation of Layered Montmorillonite

Jiang-Jen Lin,* Jiun-Chiou Wei, Tzong-Yuan Juang, and Wei-Cheng Tsai

*Institute of Polymer Science and Engineering, National Taiwan University, Taipei 10617, Taiwan*

*Received July 11, 2006. In Final Form: November 10, 2006*

Hybrids of the model BSA protein and layered silicate clay with *d* spacing of ∼62 Å were prepared from either direct or stepwise intercalation. The pristine montmorilloinite ($Na^+$-MMT) was first modified by poly(oxyalkylene)-amine salts (POP- and POE-amine) of 2000 g/mol $M_w$ to a gallery-expanded silicate (*d* spacing = 53 and 18 Å, respectively), which became accessible for BSA protein embedding. Subsequent BSA substitution allowed the embedding of the protein into the layered clay galleries in an uncompressed conformation. The stepwise process of embedding large molecules into the silicate gallery provides a new method for synthesizing biomaterial/clay hybrids potentially useful in drug delivery or biomedical design.

## Introduction

Recently, new hybrid materials involving the interaction of biomaterials with organic films,[1] organic particles,[2] and inorganic clays[3] have attracted considerable academic interests because of their unique physicochemical properties and potential applications.[4] The development of inorganic and biomaterial hybrids including proteins and nucleic acids may generate new materials with biological functions. For example, the hybrids of high-aspect-ratio layered clays with DNA were studied for new mechanism on gene transfer and cell therapy.[5] Through the adsorption or space-limitation on solid surfaces, the biomaterials may be modified for biomedical and environmental applications.[6] The strong interaction of biomaterials with inorganic surfaces may also immobilize the biomaterials including enzymes and bring up new catalytic functions through their secondary structure changes.[7] More specifically, the interaction of proteins with the naturally occurring clays has been intensively reported.[8−10] The adsorption of proteins on silicates is influenced by many factors including clay ion exchange capacity, surface area, ionic species, protein's size, and isoelectric properties.[8] It has been demonstrated that large biopolymers with positive, neutral, or negative charge may be intercalated into layered gallery of smectic clays.[9] The intercalation could improve their stability or promote new functions through the silicate platelet protection.[5] It becomes an important issue to develop a method of embedding large biomolecules in an expanded clay while retaining their original conformations and biological functions.

On the other hand, there is a great deal of research on the organic modification of naturally occurring clays for the purpose of preparing polymer nanocomposites.[11] Generally, the sodium $Na^+$-MMT clay can be exchanged with alkyl ammonium quaternary cations with a basal spacing expansion up to 40 Å.[11,12] Recently, we have revealed the use of high-molecular-weight polyoxypropylene (POP)-backboned di-quaternary salts as intercalating agents to widen the clay gallery in the range of 58−92 Å.[13] Furthermore, it was uncovered that the clay gallery expansion may proceed through a stepwise mechanism governed by the critical concentration of incorporating hydrophobic organics.[13c] These findings prompted us to explore the possibility of embedding large-molecular-weight proteins into the silicate interlayer. Here, we report the details of intercalation profile and mechanism by using a model protein, BSA, and different clay species including $Na^+$-MMT, $H^+$-MMT, and the POP-amine-modified MMT.

## Experimental Section

**Materials.** The bovine serum albumin (BSA) (Sigma) in crystalline form is of equilateral triangle shape with 14 nm width and 4 nm height.[14] In solution, BSA has an isoelectric point (pI) of 4.8, at which the zwitterion is balanced with positive and negative charges.[15] Sodium montmorillonite ($Na^+$-MMT), supplied by Nanocor Co., has a cation exchange capacity (CEC) of 120 mequiv/100 g and surface area of 750 $m^2$/g. Poly(oxyalkylene)-diamines (POA-amine) such as poly(oxyethylene) (POE)- and poly(oxypropylene) (POP)-backboned diamines, are commercially available products from Huntsman Chemical Co. Their chemical structures are illustrated in Figure 1.

* Corresponding author. Fax +886-2-3366-5237. E-mail: jianglin@ntu.edu.tw.

(1) Lvov, Y.; Ariga, K.; Ichinose, I.; Kunitake, T. *J. Am. Chem. Soc.* **1995**, *117*, 6117−6123.

(2) (a) Liu, Y. L.; Hsu, C. Y.; Su, Y. H.; Lai, J. Y. *Biomacromolecules* **2005**, *6*, 368−373. (b) Mohammed, J.; Meziani; Sun, Y. P. *J. Am. Chem. Soc.* **2003**, *125*, 8015−8018.

(3) (a) Wang, Q.; Gao, Q.; Shi, J. *J. Am. Chem. Soc.* **2004**, *126*, 14346−14347. (b) Choy, J. H.; Kwak, S. Y.; Park, J. S.; Jeong, Y. J.; Portier, J. *J. Am. Chem. Soc.* **1999**, *121*, 1399−1400.

(4) Mikhaylova, M.; Kim, D. K.; Berry, C. C.; Zagorodni, A.; Toprak, M.; Curtis, A. S. G.; Muhammed, M. *Chem. Mater.* **2004**, *16*, 2344−2354.

(5) Choy, J. H.; Kwak, S. Y.; Jeong, Y. J.; Park, J. S. *Angew. Chem., Int. Ed.* **2000**, *39*, 4041−4045.

(6) (a) Dumat, C.; Quiquampoix, H.; Staunton, S. *Environ. Sci. Technol.* **2000**, *34*, 2985−2989. (b) Zhou, Y.; Hu, N.; Zeng, Y.; Rusling, J. F. *Langmuir* **2002**, *18*, 211−219. (c) Kelleher, B. P.; Oppenheimer, S. F.; Kingery, W. L.; Han, F. X.; Willeford, K. O.; Simpson, M. J.; Simpson, A. J. *Langmuir* **2003**, *19*, 9411−9417. (d) Shchukin, D. G.; Sukhorukov, G. B.; Price, R. R.; Lvov, Y. M. *Small* **2005**, *1*, 510−513.

(7) Baron, M. H.; Revault, M.; Servagent-Noinville, S.; Abadie, J.; Quiquampoix, H. *J. Colloid Interface Sci.* **1999**, *214*, 319−332.

(8) Causserand, C.; Kara, Y.; Aimar, P. *J. Membr. Sci.* **2001**, *186*, 165−181.

(9) (a) De Cristofaro, A.; Violante, A. *Appl. Clay Sci.* **2001**, *19*, 59−67. (b) Naidja, A.; Huang, P. M.; Bollag, J. M. *J. Mol. Catal. A: Chem.* **1997**, *115*, 305−316.

(10) Lvov, Y.; Ariga, K.; Ichinose, I.; Kunitake, T. *J. Am. Chem. Soc.* **1995**, *117*, 6117−6123.

(11) Giannelis, E. P. *Adv. Mater.* **1996**, *8*, 29−35.

(12) Fu, X.; Qutubuddin, S. *Polymer* **2001**, *42*, 807−813.

(13) (a) Lin, J. J.; Chen, I. J.; Wang, R.; Lee, R. J. *Macromolecules* **2001**, *34*, 8832−8834. (b) Chou, C. C.; Shieu, F. S.; Lin, J. J. *Macromolecules* **2003**, *36*, 2187−2189. (c) Lin, J. J.; Chen, I. J.; Chou, C. C. *Macromol. Rapid Commun.* **2003**, *24*, 492−495. (d) Chou, C. C.; Chang, Y. C.; Chiang, M. L.; Lin, J. J. *Macromolecules* **2004**, *37*, 473−477.

(14) Musale, D. A.; Kulkarni, S. S. *J. Membr. Sci.* **1997**, *136*, 13−23.

(15) Cao, C. X.; Zhang, W.; Qin, W. H.; Li, S.; Zhu, W.; Liu, W. *Anal. Chem.* **2005**, *77*, 955−963.

10.1021/la062013h CCC: $37.00 
Published on Web 12/24/2006

Hydrophobic Amines

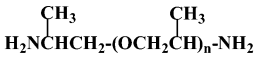

n = 33 ($M_w$ = 2000; POP-D2000)

Hydrophilic Amine

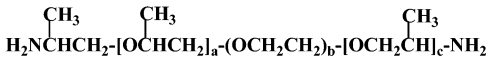

a+c = 5, b = 39.5 ($M_w$ = 2000; POE-D2000)

**Figure 1.** Chemical structures of hydrophobic poly(oxypropylene)- and hydrophilic poly(oxyethylene)-diamines.

**Preparation of POA-Amine and Acid-Treated MMT.** The preparation of the POP2000- and POE2000-intercalated MMT has been reported previously.[13] The acid-treated clay, $H^+$-MMT, was prepared according to the following procedures. $Na^+$-MMT (120 mequiv/100 g, 10 g) was vigorously stirred in 1 L of deionized water at 80 °C for several hours until completely swelled. The aqueous hydrochloric acid (37%, 2.27 g, 23 mmol) was poured into the swelled $Na^+$-MMT slurry. The mixture was continuously stirred for 24 h and then allowed to cool to room temperature. The precipitates were filtered, collected, and washed thoroughly with several portions of deionized water to remove free HCl, and then dried in a vacuum oven at 80 °C for 24 h. The X-ray diffraction analyses showed *d* spacings of 53, 18, and 15 Å for POP2000/MMT, POE2000/MMT, and $H^+$-MMT, respectively.

**Adsorption and Intercalation of BSA.** The general procedures for the organic intercalation were performed by adding the BSA solutions at pH 7 or 4 to the swelled clay suspension in water. A phosphate buffer (pH 7) and formic acid buffer (pH 4) of final concentration of 0.01 M in $H_2O$ were used. The suspensions of 30 mg/mL of BSA and 15 mg/mL of the MMT were prepared as the stock solutions. The buffer solution, the MMT (4 mL, 15 mg/mL), and BSA at varied volume (2−8 mL) were introduced in that order into a beaker, and the final volume was kept at 40 mL. The pH 4 or 7 of the suspensions with the protein/clay (w/w) ratios of 1, 2, 3, and 4 was mixed and maintained at 4 °C for 24 h. The suspensions were then centrifuged for 10 min at 10 000 rpm and washed twice (10 mL) with distilled water.

**Instruments and Analyses.** The protein concentration in the supernatant was measured by UV spectrophotometry at $\lambda = 280$ nm according to a standard curve. The amount of BSA adsorbed per gram of MMT was calculated by the difference of the BSA concentration before and after the process, and the temperature effect on the POP2000 solubility and the aggregation of the POP2000-intercalated MMT were determined with a Jasco V-530 UV−visible spectrophotometer by measuring their transmittance at 550 nm wavelength. The XRD patterns were obtained with a powder diffractometer (Schimadzu SD-D1 using a Cu target at 35 kV, 30 mA). The *d* spacing was calculated according to the Bragg's equation ($n\lambda = 2d \sin \theta$). The TGA patterns were obtained with a thermal gravimetric analysis (Perkin-Elmer Pyris 1) by heating the samples from 100 to 850 °C at 10 °C/min in air. The morphology of the BSA/MMT hybrids was analyzed by dynamic mode atomic force microscopy (DFM) and transmission electron microscopy (TEM). The DFM used was an SPA-400HV with an SPI3800N controller (Seiko Instruments Industry Co., Ltd.). The cantilever used was fabricated from Si with a spring constant of 40 N/m and a resonance frequency of 320 kHz. Transmission electron microscopy was performed on a Zeiss EM 902 A operated at 80 kV.

## Results and Discussion

**Effect of pH on the BSA Intercalation.** The BSA protein was reported to have a strong adsorption on the $Na^+$-MMT clay particles with a large surface area.[16] The adsorptive capacities are influenced by several parameters including pH environment, nature of modified clays, and stoichiometric ratios between BSA and MMT. As shown in Table 1, the effect of pH on the amounts of BSA adsorbed on MMT is demonstrated. The pristine $Na^+$-MMT and its 2000 $M_w$ amine-modified MMT (POP2000/MMT) were allowed to interact with BSA at pH 4 and 7, which is either below or above the BSA isoelectric point (pI) of 4.8. The adsorption may occur on the external surfaces and the interlayer spaces of MMT. It was found that the amounts of BSA adsorption were significantly increased at the lower pH, for example, 640 and 660 mg at pH 4, and 80 and 180 mg at pH 7 per gram of the pristine and modified MMT, respectively. The result is explained by the complimentary noncovalent forces between the charged protein and the negatively charged surface on MMT platelets. The strong electrostatic interaction of $\equiv SiO^-$ on silicates and $BSA^+$ species has resulted in the silicate/protein adsorption. At pH > 4.8 pI, BSA is mostly negatively charged ($-COO^-$), which is ineffective for exchanging with the same charges on the MMT surface.

**Table 1. Relative Adsorption Ability of BSA on $Na^+$-MMT or POP2000/MMT at Different pH Values**

| BSA/MMT[a] = 2/3 | $Na^+$-MMT | | POP2000/MMT | |
|---|---|---|---|---|
| | pH 4 | pH 7 | pH 4 | pH 7 |
| BSA adsorption (mg/g MMT) | 640 | 80 | 660 | 180 |
| adsorbed (%)[b] | 96 | 12 | 99 | 27 |

[a] Weight ratio of BSA to MMT as the starting materials. [b] On the basis of BSA (40 mg) added in aqueous solution (40 mL).

**Direct Intercalation of BSA with $Na^+$-MMT and Acid-Treated $H^+$-MMT.** The fact of incorporating BSA with $Na^+$-MMT smoothly at pH 4 but poorly at pH 7 has limited the process scope and applications. In the attempt to extend the pH scope for applications and the understanding of intercalating mechanism, $Na^+$-MMT was treated with aqueous HCl to convert into $H^+$-MMT. The acidification altered the nature of clay ionic species and slightly changed its layered structure to 15 Å *d* spacing from 12 Å for $Na^+$-MMT. By using the acidified MMT, the direct BSA intercalation is possibly performed at pH 7. Under the neutral solution, the protein intercalated into the gallery of $H^+$-MMT with the expansion of the *d* spacing to 21−33 Å (Table 2). At pH 7 (higher than pI), the protein is negatively charged ($-COO^-$) with additional amino functionalities ($-NH_2$). The basic amines tend to react with $H^+$-MMT to form quaternary ammonium salts and consequently undergo the intercalation. Yet the results indicated a low degree of XRD *d* spacing or compressed BSA conformation as conceptually illustrated in Scheme 1. For the $Na^+$-MMT intercalation, in the literature, it was shown that the BSA could be embedded into the layered silicates at 24 Å basal spacing.[9a] Our studies now demonstrate the intercalation actually depends on the amount of BSA to clay. By increasing the amount of BSA in the range of BSA/$Na^+$-MMT (weight ratio) = 1/1, 2/1, 3/1, and 4/1, the silicate *d* spacing was 48, 54, 59, and 62 Å, respectively (Figure 2 and Table 2). For comparison, the intercalation mechanism of $H^+$-MMT at pH 7 involves an ionic bridge formation rather than the conventional amine-salts/sodium ions exchange, as the intercalation of BSA (at pH 4) with $Na^+$-MMT. The results of BSA/$H^+$-MMT intercalation could only achieve a low XRD *d* spacing of 21, 25, 30, and 33 Å with different BSA loadings of 1/1, 2/1, 3/1, and 4/1 weight ratios. As summarized in Table 2 and Figure S1,

(16) Ray, S. S.; Okamoto, M. *Prog. Polym. Sci.* **2003**, *28*, 1539−1641.

**Scheme 1. Conceptual Illustration of BSA Intercalation into $Na^+$-MMT (Via the Direct Method and POP2000 or POE2000-Enlarged *d* Spacing Methods), and the Acidified MMT but at Different pH Conditions**

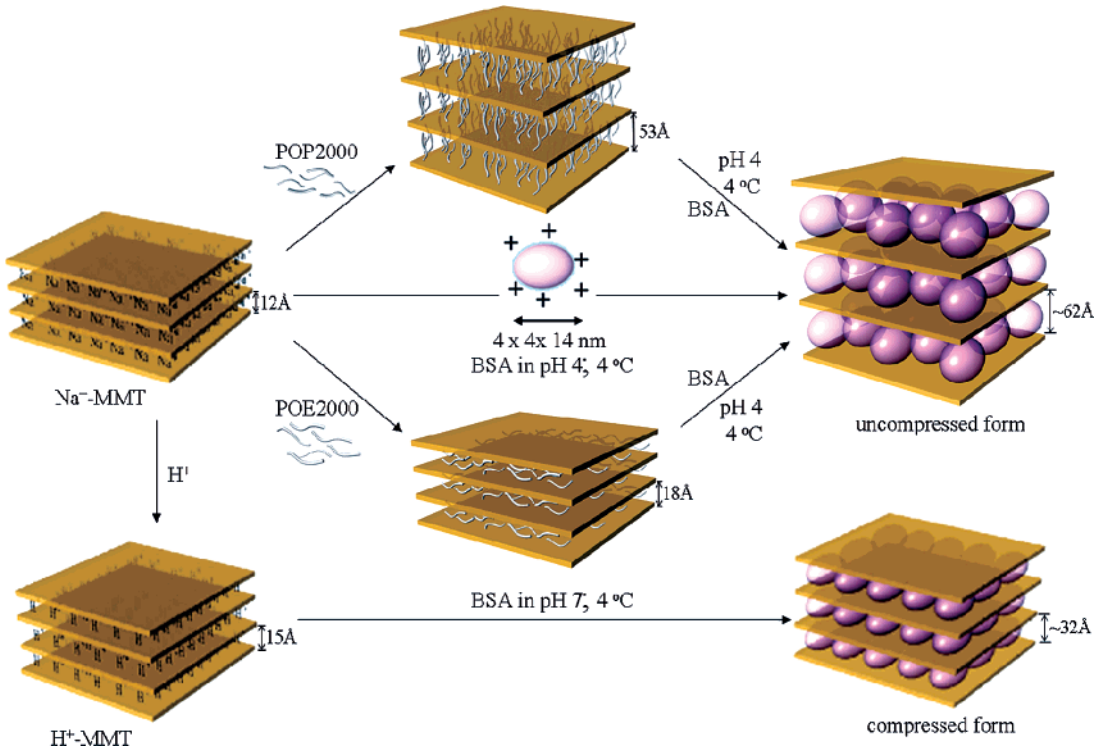


**Table 2. Embedding of BSA into Layered Silicates with and without the POP- or POE-Amine Modifications**

| | BSA adsorption | | weight fraction (org/inorg) | | |
|---|---|---|---|---|---|
| weight ratio of BSA/MMT[a] | adsorbed (mg/g MMT) | adsorbed (%) | adsorbed[c] | actual[d] | *d* spacing XRD (Å)[b] |
| | | $H^+$-MMT (15 Å) at pH 7 | | | |
| 1/1 | 290 | 29 | 23/77 | 20/80 | 21 |
| 2/1 | 430 | 22 | 30/70 | 22/78 | 25 |
| 3/1 | 500 | 17 | 33/67 | 24/76 | 30 |
| 4/1 | 770 | 19 | 44/56 | 30/70 | 33 |
| | | $Na^+$-MMT (12 Å) at pH 4 | | | |
| 1/1 | 860 | 86 | 46/54 | 50/50 | 48 |
| 2/1 | 1300 | 63 | 56/44 | 63/37 | 54 |
| 3/1 | 2200 | 74 | 68/32 | 65/35 | 59 |
| 4/1 | 2400 | 59 | 70/30 | 67/33 | 62 |
| | | POP2000/MMT (53 Å) | | | |
| 1/1 | 940 | 94 | 49/51 | 57/43 | 24 |
| 2/1 | 1600 | 80 | 62/38 | 63/37 | 51 |
| 3/1 | 2500 | 84 | 72/28 | 68/32 | 57 |
| 4/1 | 2900 | 72 | 72/28 | 68/32 | 61 |
| | | POE2000/MMT (18 Å) | | | |
| 1/1 | 980 | 98 | 50/50 | 52/48 | 24 |
| 2/1 | 1600 | 81 | 62/38 | 60/40 | 58 |
| 3/1 | 1600 | 55 | 62/38 | 60/40 | 62 |
| 4/1 | 2100 | 51 | 67/33 | 62/38 | 62 |

[a] Experiments were performed by using 3 mg/mL MMT and the corresponding amount of BSA weight. [b] XRD $n = 1$ basal spacing is calculated according to the Bragg's equation ($n\lambda = 2d \sin\theta$). [c] Weight ratios of BSA to MMT based on the BSA concentration in aqueous solutions. [d] Based on TGA measurements.

these data may be the results of the BSA intercalation plus the protein adsorption onto the external surface of the silicates. With the estimated size[14] of 4 × 4 × 14 $nm^3$ for BSA, the dimension is inconsistent with the interlayer space that was observed by XRD analyses (approximately 23 Å or *d* spacing 33 Å minus the platelet thickness[13b]). Hence, it is assumed that the BSA was embedded in a compressed conformation. In contrast, the results of 62 Å for the BSA/$Na^+$-MMT hybrids could then accommodate the BSA protein in the confinement (62 − 10 = 52 Å) without any compression.

**Requirement of Low Temperature for Stepwise Intercalation.** Besides the direct intercalation with MMT, a stepwise process is developed by first embedding POP-amine salts into the layered silicate with a 53−58 Å *d* spacing and then proceeding with the second-step BSA replacement. It was noticed that the MMT after the embedment with POP2000 had shifted its hydrophilic property to hydrophobic. The commercially available POP-diamine (2000 g/mol $M_w$) is insoluble in water due to its hydrophobic POP-backbone (Figure 1). This POP-diamine has a character of lower critical solution temperature (LCST)[17] below the ambient temperature, measured by the optical absorption at 550 nm at the concentration of 3 mg/mL in water. The LCST

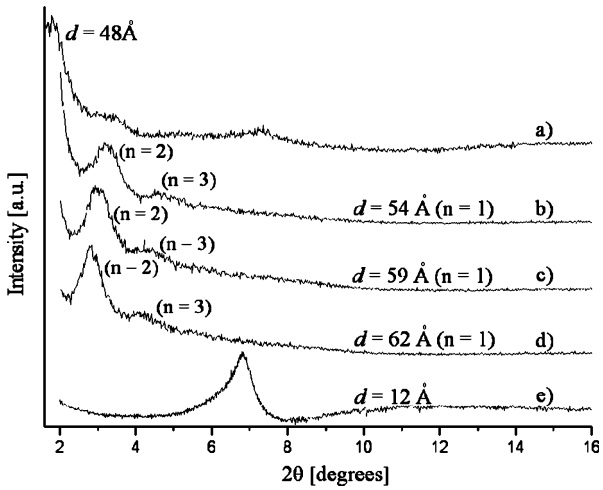


**Figure 2.** X-ray diffraction patterns of the BSA-intercalated MMT, (a) BSA/MMT = 1/1, (b) BSA/MMT = 2/1, (c) BSA/MMT = 3/1, (d) BSA/MMT = 4/1, prepared from the direct intercalation of (e) $Na^+$-MMT at pH 4.

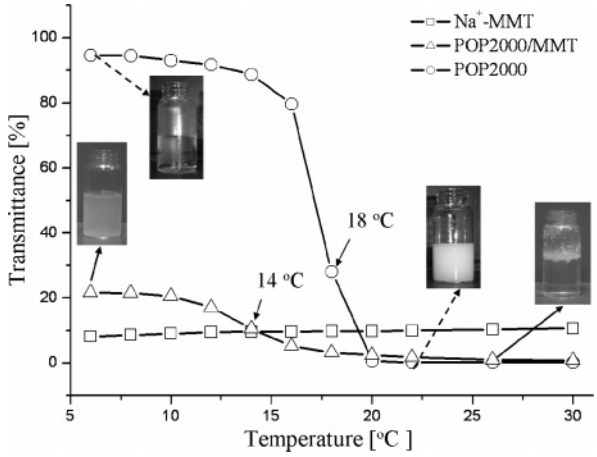


**Figure 3.** Phenomena of lower critical aggregation temperature of the POP2000-modified MMT, $Na^+$-MMT, and POP2000-diamine.

property was found by plotting its solution transmittance (%) against the temperature in the range of 5−30 °C. As shown in Figure 3, POP2000 has a critical solubility at 18 °C, above which the solubility decreases substantially. The POP2000-embedded hybrid (POP2000/MMT, *d* spacing 53 Å) is actually insoluble but dispersible in water with an inverse temperature factor behavior. The hybrid has a tendency to aggregate at ambient temperature but is well-dispersed at low temperature. The property of lower critical aggregation temperature (abbreviated as LCAT) was determined by measuring its changes of transmittance in water. The dramatic change of its transmittance was found to be around 14 °C. The change of aggregation was also visible by naked eyes and shown in the inset pictures in Figure 3. For comparison, the suspension of $Na^+$-MMT in water failed to show a critical aggregation, and a constant transmittance remained throughout the range from 6 to 30 °C. The presence of POP components affecting the hydrogen bonding with water at varied temperature is essential for demonstrating a LCAT character. It is noteworthy that the LCAT phenomena are a reversible process; in other words, the critical solubility experiments can be performed repetitively. The result indicates that the temperature for the intercalation of the POP-modified clays with proteins should be lower than 14 °C, preferably at 4 °C.

**Stepwise Intercalation of BSA into the POP-Modified MMT.** As illustrated in Scheme 1, both direct and stepwise intercalation of $Na^+$-MMT by BSA could obtain similar protein embedding XRD results. The incorporation of BSA onto the POP2000/MMT hybrids was performed at low temperature to afford the hybrids of 24, 51, 57, and 61 Å *d* spacing by using the BSA to MMT weight ratios of 1/1, 2/1, 3/1, and 4/1, accordingly (Table 2 and Figure 4). At low BSA concentration, the spacing actually shrunk and became narrower than the pristine POP2000/MMT, implying the intercalation profile may proceed with a stepwise process. With the high BSA weight ratio intercalation, the resultant XRD patterns exhibit a series of Bragg peaks including $n = 2$, 3, and 4, indicative of ordered silicate structures after the BSA intercalation. For comparison, the two-step process involving the BSA exchanging with POP2000/MMT was experimentally more reproducible to yield the hybrids with the ordered Bragg's patterns. To further understand the intercalating mechanism, the hydrophilic POE2000 intercalated clay (POE2000/MMT at 18 Å) was applied to exchange with BSA. The resultant hybrids have *d* spacings of 24, 58, 62, and 62 Å

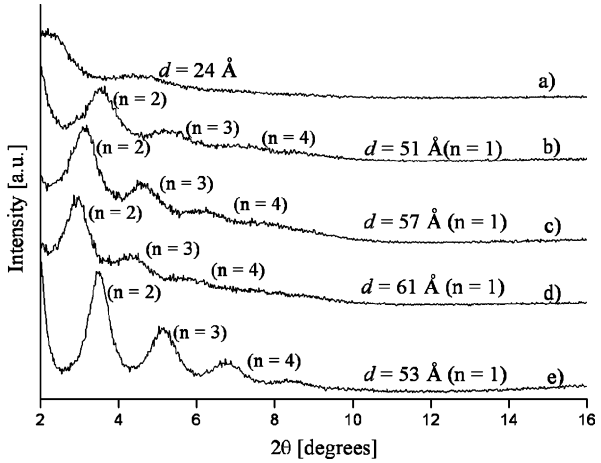


**Figure 4.** X-ray Bragg's patterns of the BSA-intercalated MMT, (a) BSA/MMT = 1/1, (b) BSA/MMT = 2/1, (c) BSA/MMT = 3/1, (d) BSA/MMT = 4/1, prepared from (e) POP2000/MMT at pH 4.0.

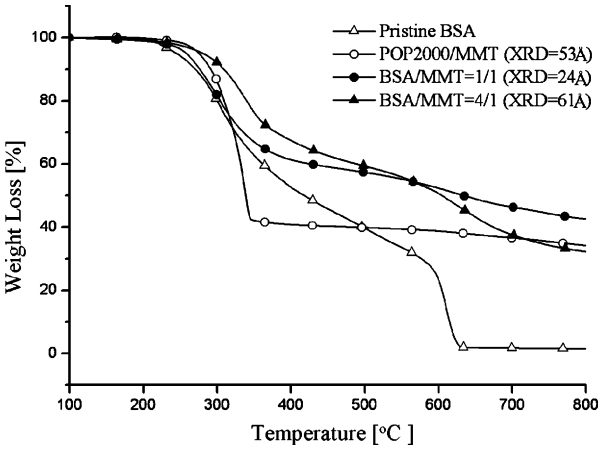


**Figure 5.** Thermo-oxidative patterns of BSA-intercalated MMT hybrids in comparison with the pristine BSA and POP2000/MMT.

by increasing the BSA amounts at 1/1, 2/1, 3/1, and 4/1 weight ratios (Table 2 and Figure S2). With the increasing protein concentration, the intercalation to MMT resulted in a sudden increase of the *d* spacing and reached 62 Å. For BSA intercalation, the uncompressed (48−62 Å) conformations can be obtained by exchanging with the hydrophobic POP2000- or hydrophilic POE2000-intercalated MMT.

**Thermal Stability of BSA in Silicate Galleries.** The thermal degradation patterns from TGA have evidenced the presence of BSA in the MMT interlayer confinement. In Figure 5, BSA itself exhibits at least two different degrading rates in the temperature ranges of 200−400 and 550−650 °C. The pattern is similar to that of BSA intercalated MMT, but different from its precursor, POP2000-MMT. The POP2000 in the clay has only a single decomposition slope around 250−350 °C. Judging from the TGA data, the amount of BSA composition in the BSA/MMT 4/1 hybrid is consistent with the estimated amounts from the solution adsorption method using UV measurements (68/32 vs 72/28 organic/inorganic ratio). In some cases, the actual TGA has a higher organic content than that calculated on the basis of the BSA remaining in solution. For example, the intercalation of BSA with POP2000/MMT afforded an organic/silicate fraction of 57/43 (w/w) in contrast to 49/51 (w/w), calculated from the solution UV absorption method (Table 2). The difference actually implies that the TGA organics includes the POP2000 component in the clay; in other words, the POP exchange reaction is

(17) (a) Gil, E. S.; Hudson, S. M. *Prog. Polym. Sci.* **2004**, *29*, 1173−1222. (b) Mao, H.; Li, C.; Zhang, Y.; Bergbreiter, D. E.; Cremer, P. S. *J. Am. Chem. Soc.* **2003**, *125*, 2850−2851.

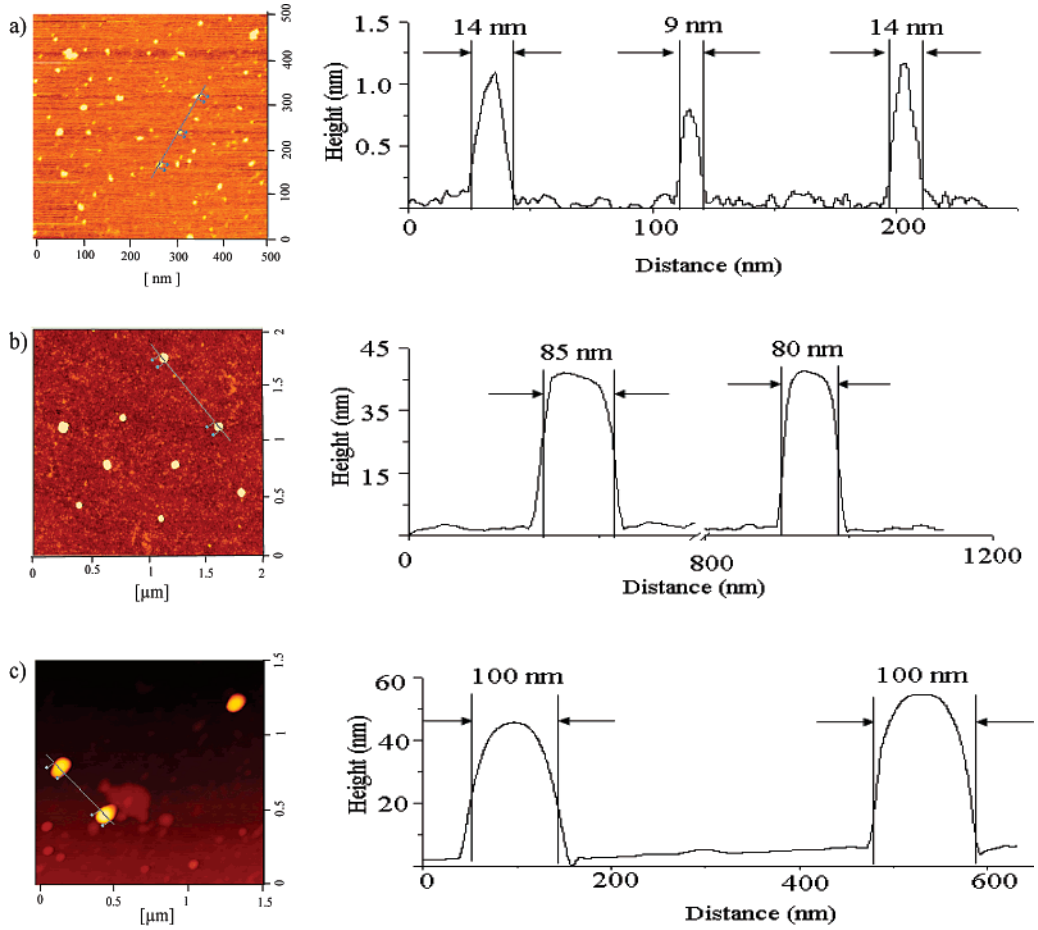


**Figure 6.** DFM topographical images of BSA-intercalated MMT and their precursors, (a) BSA on mica surface, (b) POP2000/MMT (XRD = 5.3 nm) on glass, (c) BSA/MMT (XRD = 6.1 nm) on glass.

incomplete particularly in the case of using a low concentration of BSA for intercalation.

**Direct Observation of BSA/MMT Hybrid by AFM and TEM.** After the exchange reaction, the BSA/MMT hybrid has a diverted dispersing property from that of POP/MMT. The BSA intercalated clays exhibited none of the inverse temperature factor (LCAT) after the substitution of POP components by BSA. A fine dispersion in water in the temperature range from 4 to 30 °C for the BSA/MMT hybrids can be considered as evidence for the BSA intercalation into clay. The fine dispersion allows the direct observation of their primary hybrid units. By being dispersed in water homogeneously, spin-coated on mica substrate, and dried, the primary particles can be observed by using a DFM analysis. First, the BSA image was shown in Figure 6a, by using a DFM topographical analysis, to have a base dimension of 9−14 nm width and approximately 1−4 nm height, which is a reasonable size in reference to its crystalline structure of $4 \times 4 \times 14$ nm$^3$. For the fundamental clay dimension, POP2000/MMT (53 Å XRD *d* spacing) exhibits an average height of 40−42 nm from the topographical imaging (Figure 6b). The approximate calculation amounts to 42 nm (5.3 nm *d* spacing times the height of 8−10 platelets in a stack). The number of 8−10 platelets in a stack as the primary MMT unit was previously revealed.[13b] For the BSA/MMT hybrids, which were exchanged from POP2000/MMT, the primary structure is shown to be 50−60 nm in height and 100 nm in width (Figure 6c). The height of 50 nm is also consistent with the XRD analysis (61 Å or 6.1 nm *d* spacing times 8−10 platelets). The width is also consistent with the primary unit of a platelet of average 80−100 nm[13b] for MMT. The two hybrids, BSA/MMT (XRD = 61 Å) and POP2000/MMT (XRD = 53 Å), were examined by TEM analysis (Figure S3), which shows the layered secondary structure and interlayer spacing around 60 and 50 Å. The differentiation for these primary units by TEM is rather difficult due to the limitation of the TEM scale.

## Conclusion

The BSA model protein was allowed to directly intercalate into $Na^+$-MMT (12 Å XRD basal spacing) by using an excess amount of BSA or exchange with the spatially expanded POP2000/MMT (53 Å). The stepwise intercalation involving the POP/MMT hybrids required a low temperature below the LCAT (14 °C) to avoid the clay aggregation in water. Both processes could afford the uncompressed BSA in the clay galleries (62 Å). When using $H^+$-MMT, the BSA intercalation can only achieve a low *d* spacing of 33 Å. The TGA data exhibited a higher thermal stability for BSA in the silicate confinement, providing evidence for the BSA embedment. The existence of the BSA/MMT and POP2000/MMT primary units was observed by using DFM. The newly developed process for encapsulating BSA could lead to the formation of biopolymer/clay hybrids, potentially useful for biomedical applications.

**Acknowledgment.** We acknowledge financial support from the National Science Council (NSC) of Taiwan.

**Supporting Information Available:** XRD of BSA intercalation into $H^+$-MMT and POE2000/MMT, and TEM micrographs. This material is available free of charge via the Internet at http://pubs.acs.org.

LA062013H